

Parametric excitation and chaos through dust-charge fluctuation in a dusty plasma

Madhurjya P Bora and Dipak Sarmah
*Physics Department, Gauhati University, Guwahati, India.**

We consider a van der Pol-Mathieu (vdPM) equation with parametric forcing, which arises in a simplified model of dusty plasma with dust-charge fluctuation [1]. We make a detailed numerical investigation and show that the system can be driven to chaos either through a period doubling cascade or through a subcritical pitchfork bifurcation over an wide range of parameter space. We also discuss the frequency entrainment or frequency-locked phase of the dust-charge fluctuation dynamics and show that the system exhibits 2:1 parametric resonance away from the chaotic regime.

I. INTRODUCTION

The subject of parametric excitation can be traced back to Faraday in 1831 [2], when he observed that surface waves in a fluid-filled cylinder under vertical excitation exhibited twice the period of the excitation itself. The most simplified version of parametric excitation was given by Mathieu in 1868 [3] related to the vibrations of an elliptical membrane, which now has become a model equation for response of many systems to sinusoidal parametric excitation. The simplest Mathieu equation can be stated as [4],

$$\ddot{x} + (\delta + \epsilon \cos t)x = 0, \quad (1)$$

with δ and ϵ as constants. There have been extensive investigations of parametric excitation and resonance related Mathieu equation by several authors [5, 6, 7]. One of the very common examples of parametric forcing modeled by the nonlinear Mathieu equation is the forced and unforced inverted pendulum [8].

In this work, we have studied the parametric excitation and resonance of the van der Pol-Mathieu (vdPM) equation, which arises in a simplified model of dusty plasma with dust-charge fluctuation. Dusty plasmas are characterized by presence of massive dust (impurities) particles embedded in an electron-ion plasma [9]. Immersed in the plasma, the dust particles acquire charges by collecting the electrons and ions on their surfaces, which are mostly negative. However, the charge on a dust particle is never a constant and varies temporally. Thus, along with other their dynamical properties, the charge of the dust particles becomes a dynamic variable, which can severely modify the plasma properties. The presence of dust particles in a plasma may modify the dynamics of the plasma in many ways, of which the most prominent is the appearance of low frequency dust-acoustic waves [9]. The dust-charge fluctuation is known to damp the acoustic waves in a dusty plasma [9, 10]. Recently, Momeni, Kourakis, and Shukla [11] has studied a simplified model of nonlinear dust-charge fluctuation based on a vdPM equation, where they have discussed the stability regions of the vdPM equation and have shown the existence of stable and unstable periodic orbits in different parameter space. This vdPM equation is originally derived by Saitou and Honzawa [1], where they have shown that in a very restricted region of parameter space, the system exhibit chaotic behavior. They argue that the oscillations leading to chaos basically stems out of the balancing between the van der Pol (vdP) and Mathieu-like terms.

We report, in this paper, a detailed investigation of the vdPM equation for dust-charge fluctuation and show that the vdPM equation proposed by Saitou [1] can exhibit chaotic behavior over an wide range of relevant parameter space, which is, in many instances, preceded by period doubling cascades. We have found that both period doubling and pitchfork bifurcations take place as one varies the bifurcation parameters, both leading to chaos. The range of parameters for a chaotic regime comes out to be not as restrictive as pointed out by Saitou [1]. We have discussed the stability and bifurcation of the nonlinear system and found that the system can be completely deterministic in between chaotic regimes. The paper is organized as follows. In Section II, we formulate the nonlinear dust-charge fluctuation model yielding the vdPM equation and discuss about the parametric forcing. In Section III, we have discussed about frequency entrainment (frequency-locked phase) of the nonlinear oscillator, driven by the parametric forcing term. We have shown that far away from the chaotic regime, the system can be driven by a 2:1 parametric resonance leading to a stable limit cycle. Away from the resonance, it displays quasi-periodic behavior. We discuss the stability and bifurcation of the periodic orbit of the nonlinear system in Section IV with the help of Floquet stability theory and show that the instability of a limit cycle may manifest through a period doubling bifurcation.

*Electronic address: mpbora@yahoo.com

In Section V, we explore the chaotic regime of the vdPM equation, where we show that the system can be driven to chaos over an wide range of parameters. We have found that the route to chaos may be through a period doubling cascade. We draw the conclusions in Section VI.

II. DUST-CHARGE FLUCTUATION MODEL

We consider an unmagnetized collisionless plasma consisting of electrons, ions, and massive dust particles, which become charged by acquiring charged particles (ion or electrons) on their surfaces. The subject of dust-charge fluctuation in a dusty plasma is a well studied process which, primarily, has a damping effect on the acoustic waves [10]. Here, we assume that the number densities of the charged particles are considerably larger than that of the dust particles, so that the effect of dust-charge fluctuation on the dynamics of the electrons and ions is negligible and charge neutrality is always satisfied [1]. So, the charge on the dust grains $q(t)$ becomes a time dependent function.

Assuming the equilibrium (unperturbed) state to be static, we can write the nonlinear continuity, momentum balance, and the Poisson equation for dust-charge fluctuation as [1, 11],

$$\frac{\partial n}{\partial t} + n_0 \nabla \cdot \mathbf{v} = \alpha n - \frac{1}{3} \beta n^3, \quad (2)$$

$$m_d \frac{d\mathbf{v}}{dt} = q\mathbf{E}, \quad (3)$$

$$\varepsilon_0 \nabla \cdot \mathbf{E} = qn, \quad (4)$$

where m_d, n_0, ε_0 are dust mass, equilibrium dust number density, and permittivity of free space. The variables $n, \mathbf{v}, \mathbf{E}$ are perturbed dust density, velocity, and electric field. In the first equation, Eq.(2), the terms on the right hand side denote the rate of production and loss of charged dust grains, where α and β are constants of proportionality. In writing these terms, we have assumed that the production rate of charged dust particles is proportional to the dust density. The cubic loss term appears mainly due to the loss of dust grains through a three-body recombination process [1]. In the momentum equation, Eq.(3), we have assumed the dust particles to be cold which basically eliminates any variant of dust-acoustic waves. In writing these equations, we have assumed that the average dust velocity, \mathbf{v} , is fairly uniform in space and its spatial gradient is considerably smaller so that the convective derivative term in the momentum equation, namely, the term $(\mathbf{v} \cdot \nabla)\mathbf{v}$ can be neglected. Further, we have approximated the term $\nabla \cdot (n\mathbf{v})$ with $n_0 \nabla \cdot \mathbf{v}$, assuming a uniform distribution of the charged dust particles in space ($\nabla n \approx 0$) [11]. We assume the dust-charge $q(t)$ to be changing harmonically with time with a frequency ν and use the ansatz [1, 11],

$$q(t) = q_0(1 - \epsilon\lambda \cos \nu t)^{1/2}, \quad (5)$$

where the term $(\epsilon\lambda)$ denotes the strength of charge fluctuation. Note that, in principle, there is no need to restrict the value of the term $(\epsilon\lambda)$ to a smaller value, which gives us freedom to explore an wider parameter space of α - ϵ .

Without loss of generality, we consider only one dimension, z and write Eqs.(2-4) as,

$$\frac{\partial n}{\partial t} + n_0 \frac{\partial v_z}{\partial z} = \alpha n - \frac{1}{3} \beta n^3, \quad (6)$$

$$m_d \frac{\partial v_z}{\partial t} = qE_z, \quad (7)$$

$$\varepsilon_0 \frac{\partial E_z}{\partial z} = qn. \quad (8)$$

By taking a z -derivative of Eq.(7), we can eliminate the terms involving perturbed velocity and electric field using Eqs.(8) and (6) to get a coupled differential equation in perturbed density,

$$\frac{d^2 n}{dt^2} - (\alpha - \beta n^2) \frac{dn}{dt} + n\omega_d^2(1 - \epsilon\lambda \cos \nu t) = 0, \quad (9)$$

where $\omega_d = (n_0 q_0^2 / m_d \varepsilon_0)^{1/2}$ is the plasma frequency corresponding to the dust particles. The above equation, Eq.(9) can be classified as *van der Pol-Mathieu* (vdPM) equation [1], owing to the nonlinear term $(\alpha - \beta n^2)$ which is like a van der Pol (vdP) term [4] and parametric forcing term $(1 - \epsilon\lambda \cos \nu t)$ which like the parametric term of a classical Mathieu equation [4].

A. Parametric forcing

As is well known from the theory of classical Mathieu equation, the parametric forcing term in Eq.(9) makes the dynamics of the dust-charge fluctuation prone to chaos [8, 12, 13, 14]. As the vdP equation has a stable limit cycle, we can see that Eq.(9) should show vdP-type behavior for large α . However the parametric forcing term may still drive the system unstable. In all probability, we expect the onset of chaotic behavior as ϵ increases, which should be more pronounced when $\alpha \ll 1$.

In absence of the parametric forcing term, the stable limit cycle of the vdP equation has frequency of 1. Another well known result from the analysis of Mathieu equation [4] is that the origin becomes unstable when the parametric forcing frequency ν is close to twice the frequency of the unforced oscillator. So, when both the vdP and Mathieu terms are present, as in Eq.(9), we expect a frequency entrainment at 2:1 [15] and the system represented by Eq.(9) must exhibit some sort of quasi-periodic and frequency-locked (entrainment) behaviors in the parameter space of ϵ - α before it can be driven to chaos. The route to chaos should be through a series of quasi-periodic regime or through a period-doubling cascade rather than the other universal route i.e. through intermittancy [16].

III. FREQUENCY ENTRAINMENT

Entrainment dynamics plays an important part in design engineering and many other dynamical systems [17]. Recently, frequency entrainment is shown to exist in nonautonomous chaotic oscillators [18]. In this work, we consider the possible entrainment by the parametric term, which can lead to quasi-periodicity and finally to chaos. We consider the following dynamical equation for this dust-charge dynamics,

$$\ddot{x} - (\alpha - \beta x^2)\dot{x} + \omega_d^2 x(1 - \epsilon \lambda \cos \nu t) = 0, \quad (10)$$

where we have replaced the dust density n by the variable x . In order to facilitate the multiple scales in the problem and entrainment, we assume that $\alpha \sim \beta = \delta \ll 1$, a small number. As the entrainment is possible only when the system is far away from the chaotic regime, when ϵ is small, we assume that $\epsilon < 1$. We further re-scale the time by $t \rightarrow \omega_d t$ and write Eq.(10) as

$$\ddot{x} - \mu \epsilon (1 - x^2)\dot{x} + x(1 - \epsilon \lambda \cos 2\omega t) = 0, \quad (11)$$

where $\mu \epsilon = \delta/\omega_d$. The strength of the parametric forcing term is given by $\epsilon \lambda$ with $\epsilon < 1$ and $\nu = 2\omega$. We expect that the parametric forcing should result in a 2:1 subharmonic resonance, when the parametric frequency ν is close to 2 or $\omega \sim 1$. Note that in absence of the parametric forcing term ($\epsilon \lambda = 0$), the natural frequency of the oscillator is unity.

We now introduce two different time-scales [15, 16], the stretched time $\xi = \omega t$ and the slow time $\eta = \epsilon t$ and expand the forcing frequency ω about the natural frequency of the oscillator i.e. 1 with ϵ as the expansion parameter,

$$\omega = 1 + k\epsilon + \mathcal{O}(\epsilon^2), \quad (12)$$

where k is a detuning parameter at order ϵ . The variable x now is expanded in a power series

$$x = x_0(\xi, \eta) + \epsilon x_1(\xi, \eta) + \mathcal{O}(\epsilon^2). \quad (13)$$

Substituting Eqs.(12) and (13) in Eq.(11) and collecting terms at the order $\epsilon = 0$ and 1, we have,

$$x_{0\xi\xi} + x_0 = 0, \quad (14)$$

$$, \quad (15)$$

where the subscripts refer to derivatives with respect to ξ and η . The solution to Eq.(14) can be taken as

$$x_0(\xi, \eta) = A(\eta) \cos \xi + B(\eta) \sin \xi, \quad (16)$$

where the coefficients A and B are functions of the slow time-scale. Substituting Eq.(16) into Eq.(15) and removing the secular terms [16], we have the following coupled differential equations for the slow time-scale,

$$A' = -kB + \frac{1}{2}\mu A - \frac{1}{8}\mu A(A^2 + B^2) + \frac{1}{4}\lambda B, \quad (17)$$

$$B' = kA + \frac{1}{2}\mu B - \frac{1}{8}\mu B(A^2 + B^2) + \frac{1}{4}\lambda A. \quad (18)$$

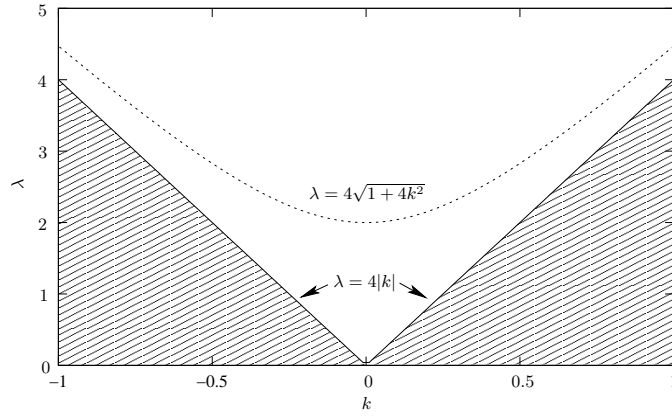


Figure 1: Bifurcation diagram of Eqs.(17) and (18) in the k - λ plane. The line $\lambda = 4|k|$ along which a Hopf bifurcation occurs at the origin. Below this line, in the shaded region, there exists a limit cycle. The dashed line denote a saddle-node bifurcation at the origin.

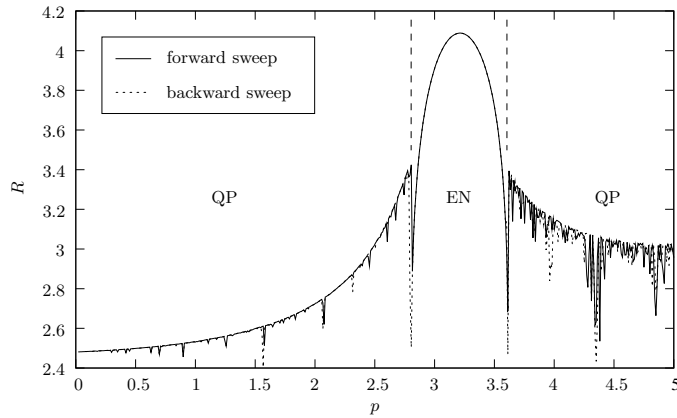


Figure 2: Entrainment by the parametric dust-charge fluctuation for $\alpha = 0.15, \beta = 0.1, \lambda = 1.0, \omega_d = 1.0, \epsilon = 0.5$, where the amplitude R of the oscillation is plotted against the period p of the parametric forcing term. The two vertical dashed lines at $p = 2.8$ and 3.6 indicate the region of entrainment (marked as EN). The other behavior is quasi-periodic (marked by QP). Only very little hysteresis is observed in the quasi-periodic regions.

We note that the hyperbolic fixed points of the slow flow correspond to the periodic motion of the original equation Eq.(11) i.e. an entrainment and limit cycles of the slow flow correspond to quasi-periodic motions of Eq.(11) [19]. From simple resonance dynamics it is evident that the entrainment region of Eq.(11) by the parametric forcing term should increase as the parametric forcing amplitude λ increases, allowing a wider range in the detuning parameter k during which the entrainment is observed. Therefore it is worthwhile to study the flow of the slow variables through Eqs.(17) and (18) as we vary the parameters k and λ .

In Fig.1, the bifurcation diagram of the slow flow in the k - λ plane is shown. Along the line $\lambda = 4|k|$, a Hopf bifurcation occurs at the origin, below which, in the shaded region, a limit cycle appears. As λ falls below $4|k|$, the fixed point at the origin becomes an unstable spiral [complex eigenvalues of the linearized Jacobian of Eqs.(17) and (18)] from an unstable node. Along the line $\lambda = 4\sqrt{1+4k^2}$, saddle node bifurcation occurs for sufficiently high λ when the origin becomes a saddle point from an unstable node after two other saddle points coalesce at the origin. From what we have observed, one can conclude that entrainment by parametric forcing occurs above the shaded region of Fig.1. In the shaded region, we expect a quasi-periodic behavior. These results are confirmed from the numerical solutions of Eq.(11), which are shown in Fig.2. The entrainment region for $\lambda = 1$ can be calculated from Fig.1 as $-0.25 < k < +0.25$, which in terms of period of Eq.(11) for the parameters of Fig.1, is given by $2.79 < p < 3.59$ which very well agrees with the numerical results (see Fig.2).

As we increase ϵ , the expansion parameter, the prediction from Fig.1 however agrees less and less as the system makes a transition to chaos.

IV. STABILITY AND BIFURCATIONS

The stability of a periodic orbit can be effectively studied using Floquet theory [19, 20]. In this section, we briefly review the Floquet theory with reference to Eq.(10). We first write the second order dynamical equation Eq.(10) as two first order equations,

$$\dot{x} = y, \tag{19}$$

$$\dot{y} = (\alpha - \beta x^2)y - \omega_d^2 x(1 - \epsilon \lambda \cos \nu t). \tag{20}$$

We have already shown in the previous section that a frequency-locked (entrained) phase with a single periodic limit cycle can exist for Eqs.(19,20). In this section, we are going to study the stability of this periodic orbit and bifurcations leading to the onset of chaos.

The Poincaré map of an initial point $z_0 = (x_0, y_0)$ on the periodic orbit (limit cycle) can be obtained by sampling the orbit points z_n at discrete time interval $t = t_n$, $n = 1, 2, 3, \dots$. So the transformation which successively maps the Poincaré section $P(z)$ is $z_{n+1} = P(z_n)$. The linear stability of a q -periodic orbit with $P^q(z_0) = z_0$ can now be determined from the linearized map given by the matrix DP^q of P^q at an orbit point z_0 , where P^q is the q -times iterated Poincaré map. The linearized matrix $M = DP^q$ can be obtained by integrating the linearized equations corresponding to Eqs.(19,20) for small perturbations along the q -periodic orbit [19].

Assume that $z^*(t) = z^*(t + q)$ is a point lying on the q -periodic limit cycle of Eqs.(19,20). We perturb the orbit with a small perturbation $\delta z = (\delta x, \delta y)$ and linearize Eqs.(19,20) about the closed orbit,

$$\begin{pmatrix} \dot{\delta x} \\ \dot{\delta y} \end{pmatrix} = J(t) \begin{pmatrix} \delta x \\ \delta y \end{pmatrix}, \quad J(t) = \begin{pmatrix} 0 & 1 \\ f_x & f_y \end{pmatrix}_{(x,y)=(x^*,y^*)}, \tag{21}$$

where $J(t)$ is the q -periodic linearized Jacobian. The partial derivatives $f_{x,y}$ are given by,

$$f_x = -2\beta xy - \omega_d^2(1 - \epsilon \lambda \cos \nu t), \quad f_y = (\alpha - \beta x^2). \tag{22}$$

We now assume that $W(t) = [w_1(t), w_2(t)]$ is a fundamental solution matrix with $W(0) = I$ [19]. The general solution of the q -periodic system, Eq.(21), is then given by,

$$\begin{pmatrix} \delta x(t) \\ \delta y(t) \end{pmatrix} = W(t) \begin{pmatrix} \delta x(0) \\ \delta y(0) \end{pmatrix}. \tag{23}$$

We then substitute Eq.(23) into Eq.(21) to obtain the initial value problem,

$$\dot{W}(t) = J(t)W(t), \quad W(0) = I, \tag{24}$$

where $W(q)$ is the linearized map $DP^q(z_0)$. So, the matrix DP^q can, in principle, be obtained from numerical integration of Eq.(24) over period q . However, the numerical procedure is not very straight forward and requires sophisticated techniques to determine the exact form of the matrix DP^q which is very sensitive to initial conditions (x^*, y^*) . The matrix DP^q is known as the *monodromy* matrix for the q -periodic orbit and the eigenvalues of this monodromy matrix, popularly known as the Floquet multipliers [19, 20], indicate the stability of the q -periodic orbit. Therefore, the values of the Floquet multipliers have to be determined with considerable precision for understanding the true nature of the stability of the nonlinear system. The characteristic equation of the linearized map $M = DP^q$ is given by,

$$\zeta^2 - \tau\zeta + \Delta = 0, \tag{25}$$

where the eigenvalues $\zeta_{1,2}$ are the Floquet multipliers and $\tau = \text{tr}(M)$, $\Delta = \det(M)$. The determinant Δ is given by [19, 20, 21]

$$\Delta = e^{\int_0^q \text{tr}(J) dt} = e^{(\alpha - \beta x^{*2})q}, \tag{26}$$

$$\tau = \frac{1}{q} \int_0^q \text{tr}(J) dt \left(\text{mod} \frac{2\pi i}{q} \right). \tag{27}$$

We know from Floquet theory that the periodic orbit is stable only if the pair of Floquet multipliers lie inside the unit circle. The bifurcations of the periodic orbit occur on the unit circle. From the expression for Δ , Eq.(26), it can be seen that we do have bifurcations depending on a balancing of the parameters α, β , and the periodic orbit, which is

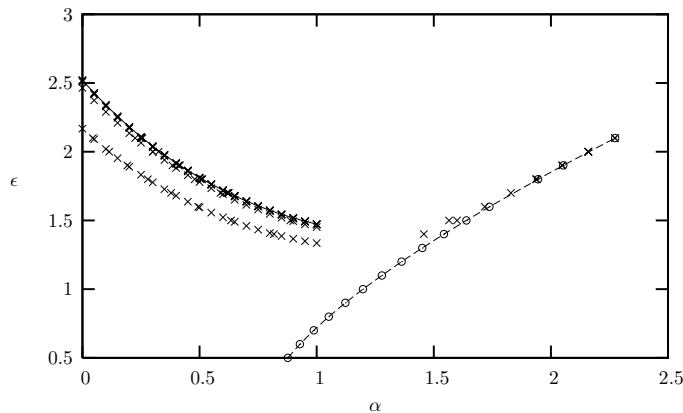


Figure 3: Stability diagram of Eqs.(19,20) in the α - ϵ plane. The period doubling bifurcations occur along the lines denoted by the points ‘ \times ’. The points denoted by a ‘ \circ ’ along the dashed line indicate pitchfork bifurcations. The chaotic regime lies above the two lines. As we can see that some pitchfork bifurcations are followed by a period doubling cascade. The other parameters are $\beta = 0.1$ and $\nu = \omega_d = \lambda = 1.0$.

Table I: Scaling of period doubling cascades.

k	α_k	δ_k	ϵ_k	δ_k
1	0.3781420		1.952855	
2	0.5888546	7.61	2.209903	6.85
3	0.6165303	4.77	2.247453	4.73
4	0.6223341	4.70	2.255401	4.70
5	0.6235698	4.67	2.257093	4.65
6	0.6238345		2.257457	

determined by the parameter ϵ , the magnitude of the parametric driving force. In all probability, the unstable region should lie in the region of large α . We numerically determine the Floquet multipliers for a range of periodic orbit in the parameter space (α, ϵ) with $\beta = 0.1$ and $\omega_d = \lambda = 1.0$ and the resultant stability diagram is shown in Fig.3. In Fig.3, period doubling bifurcations occur along the lines denoted by a ‘ \times ’ sign and subcritical pitchfork bifurcations occur along the dashed line denoted by a ‘ \circ ’. The line joining the ‘ \times ’ points in the figure denotes the accumulation points or the limiting points of the period doubling bifurcations before transition to chaos. The chaotic regime lies above these lines. As the two lines seem to intersect, when extended, we see that some of the period doubling cascades are preceded by pitchfork bifurcations.

As the pair of Floquet multipliers decreases through -1 at the period doubling points, the q -periodic orbit loses its stability to jump to a $2q$ -periodic stable limit cycle. So, in the observed parameter regime of Fig.3, all period doubling bifurcations are supercritical [16]. In case of the pitchfork bifurcations, the Floquet multipliers increases through $+1$ and are subcritical as there are no stable limit cycles after the bifurcations and the system becomes aperiodic [16]. In Figs.3(a) and (b), two successive period doubling orbits are shown. In Figs.5(a) and (b), we have shown the bifurcation diagrams with the bifurcation parameters as α and ϵ (for details, please see the captions in the figure). These bifurcation diagrams are obtained with the help of AUTO [22] as a part of the XPPAUT package [23].

A. Scaling of the period doubling cascades

It is interesting to investigate the scaling behaviour of the period doubling cascades in light of the scaling of the period doubling sequences in 1-D maps. As usually observed in any period doubling cascades, the bifurcation parameter, which in our case are α and ϵ , converges geometrically to a limiting value with the convergence ratio approaching a unique value, analogous to Feigenbaum number in case of 1-D maps [16, 24]. In Table.I, we have listed the values of the bifurcation parameters as these converge to their respective limiting values. The ratio of this convergence δ_k , expressed as,

$$\delta_k = \frac{A_k - A_{k-1}}{A_{k+1} - A_k}, \quad \lim_{k \rightarrow \infty} \delta_k = \delta, \quad (28)$$

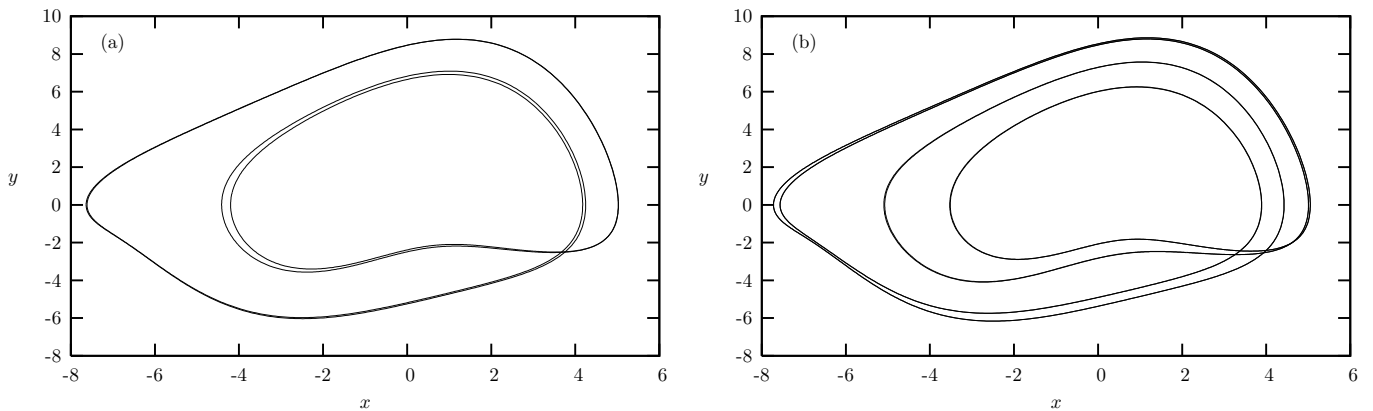


Figure 4: Phase portrait of two successive period doubling orbits for $\alpha = 0.5$ and (a) $\epsilon = 1.779955$ and (b) $\epsilon = 1.805263$. Rest of the parameters are same as in Fig.3.

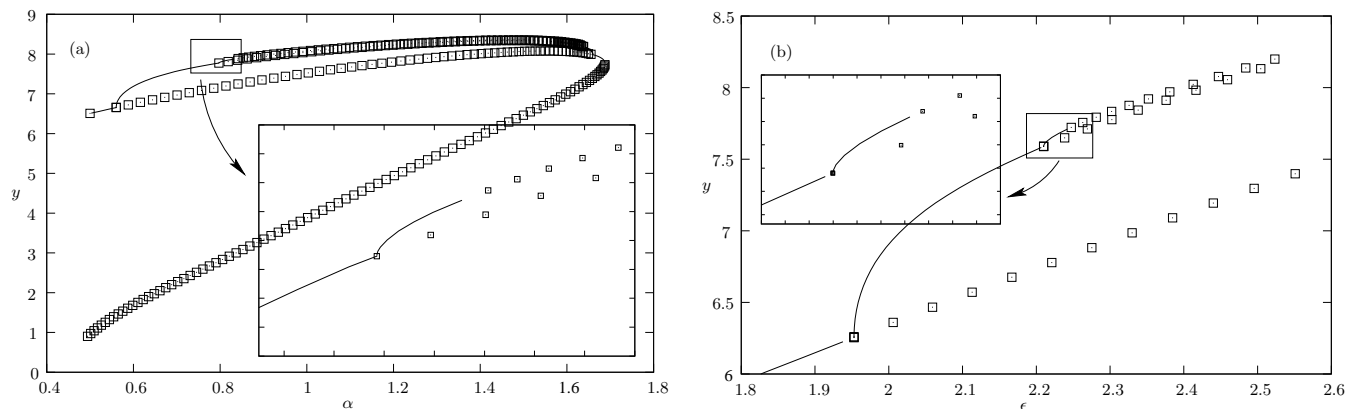


Figure 5: Bifurcation diagrams for the period doubling sequences. In (a), the bifurcation parameter is α with $\epsilon = 1.5$ and in (b), the bifurcation parameter is ϵ with $\alpha = 0.15$. All other parameters are same as in Fig.3. The *open boxes* in the diagrams are unstable orbits and the solid lines indicate stable periodic orbits (limit cycles) with period doubling bifurcations. Blow-up regions of the second period double cascade is shown in the insets.

approaches a unique limiting value δ as the bifurcation parameter $A_k \rightarrow \text{const.}$, with k denoting each successive period doubling point. The value of δ characterizes the scaling property of the bifurcation, which agrees well with the Feigenbaum number $4.669\dots$ for 1-D maps [8, 14, 24].

V. TRANSITION TO CHAOS

In this section, we study the chaotic behavior of Eq.(10). The single most prominent feature of chaos is its sensitive dependence on initial conditions, which is measured by the Lyapunov characteristic exponents (LCEs) [25]. These exponents are invariant global indicators of the non-linear system. For a continuous dynamical system described by a set of autonomous ordinary differential equations, the number of LCEs is equal to the dimension of the system. By discretizing the temporal dimension as Δt , the LCEs can be defined as,

$$\sigma_i = \lim_{N \rightarrow \infty} \lim_{\Delta t \rightarrow 0} \frac{1}{N \Delta t} \ln[S_i(M_N)], \quad (29)$$

where

$$M_N = \prod_{i=0}^N e^{J(i\Delta t)\Delta t}. \quad (30)$$

In the above relations, S_i are the singular values of the matrix M_N and J is the Jacobian. Numerically, the number N denotes the number of integration steps of length Δt . Here, we employ a numerical algorithm, based on the Wolf's

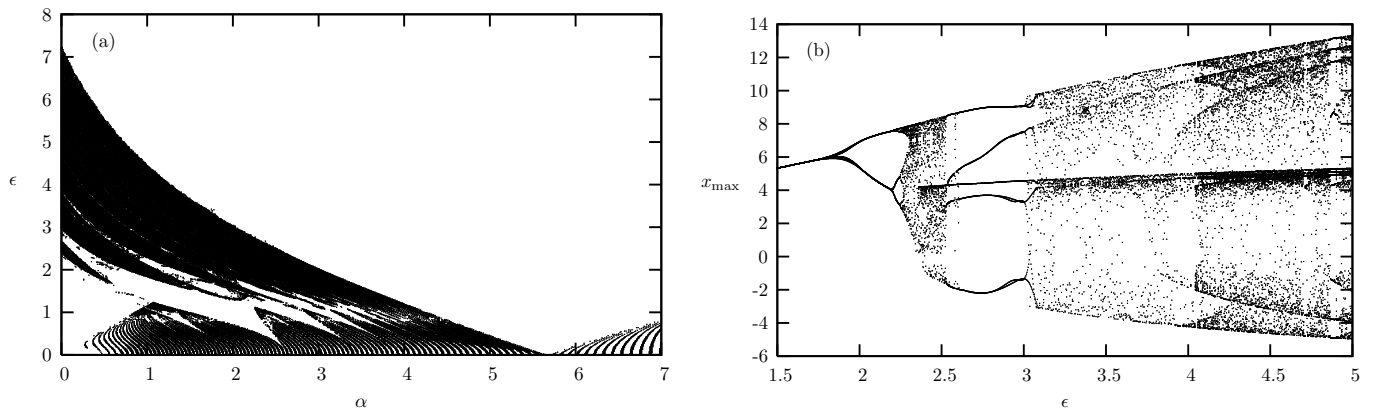


Figure 6: (a) Plot of the maximal Lyapunov exponent, σ_1 , for Eq.(10) in the parameter space of α - ϵ . The Lyapunov exponent is calculated in the entire parameter space indicated in the figure. The *blackened* portions indicate a positive and the blank portions of the figure indicate a negative Lyapunov exponent. As can be seen from the figure, the fractal nature of the chaos is indicated by repetitive appearance of the whole figure in the smaller regions close to the horizontal axis. It also seems that the entire figure is *only* a part of a large figure covering the entire α - ϵ plane. (b) The orbit diagram for Eq.(31), where the successive local maxima are plotted against the bifurcation parameter, for $\alpha = 0.15$. Other parameters are same as in (a).

well known method to calculate the LCEs [26]. Note that, Wolf's original method is not the best approach to calculate the LCEs and it can be modified to contain the non-uniformity-factors of the LCEs [27]. An important necessary step in Wolf's algorithm is to re-orthogonalize of the set of vectors, which is carried out, usually, through Gram-Schmid orthogonalization procedure. In our numerical routine too, we have used the Gram-Schmid orthogonalization to calculate the LCEs. In particular, we have calculated the LCEs for the following autonomous system,

$$\begin{aligned}
 \dot{x} &= y, \\
 \dot{y} &= (\alpha - \beta x^2)y - \omega_d^2 x(1 - \epsilon \lambda u), \\
 \dot{u} &= u(1 - u^2 - v^2) - 2\pi v/T, \\
 \dot{v} &= v(1 - u^2 - v^2) + 2\pi u/T,
 \end{aligned} \tag{31}$$

where $\nu = 2\pi/T$. Note that, we have made the original non-autonomous equation, Eq.(10), a system of autonomous equations by introducing the last two equations of Eqs.(31), which have stable and unique solutions,

$$u(t) = \cos(2\pi t/T), \quad v(t) = \sin(2\pi t/T), \tag{32}$$

for the initial values $[u(0), v(0)] = [1, 0]$.

In Fig.6(a), we have plotted the maximal LCE for the Eqs.(31), in the parameter space of α - ϵ for the range shown. The parameters are $\beta = 0.1, \omega_d^2 = 1$, and $\lambda = 1$. The period of the orbit is chosen as $T = 6.5$ which corresponds to $\nu = 0.96664$. The *blackened* portions of the figure indicate a positive Lyapunov exponent indicating chaos. In all other places the maximal Lyapunov exponent is negative, signifying stable oscillations of the system. We can see the fractal behavior of the chaos from the figure. It also seems that the whole figure is only a part of a larger figure covering the entire domain of the α - ϵ plane. In Fig.7, the maximal LCE, σ_1 , is plotted along with a blow up of the region of period doubling cascades. The period doubling points are marked with 'arrows' in Fig.7(b).

We have constructed an *orbit* diagram [16] [Fig.6(b)] for the system, Eq.(31), where we have plotted the successive local maxima for the variable x of the oscillation against the bifurcation parameter ϵ . The period doubling bifurcations occur near 1.9 and 2.2 before the system becomes chaotic. Note the appearance of 5-period window in the region $\epsilon = 2.5$ and 3.0 after which the system becomes chaotic again. The chaotic orbit along with the time evolution of the system in the chaotic regime and the Poincaré map are shown in Fig.8.

VI. CONCLUSION

In this work, we have carried out a detailed investigation of the stability, bifurcation leading to chaos for the vdPM system arising out dust-charge fluctuation in a dusty plasma. We have shown that the system can be highly chaotic depending the chosen parameters and not as restrictive as has been pointed out by Saitou and Honzawa [1]. In fact, an wide range of chaotic region exists for the parametric driving strength ($\epsilon\lambda$) as low as 0.05, as shown by the plot of

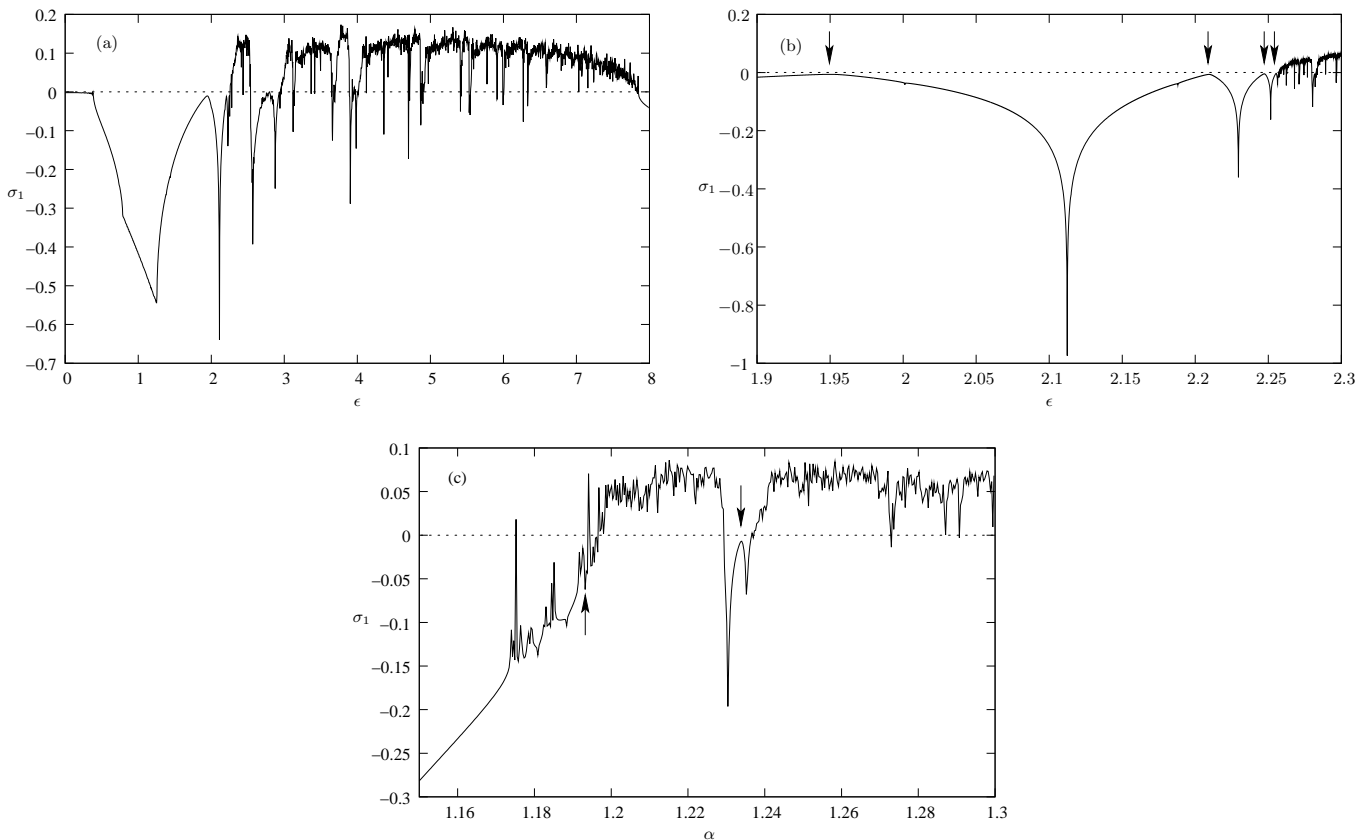


Figure 7: (a) Plot of the maximal Lyapunov exponent σ_1 against the bifurcation parameter ϵ for $\alpha = 0.15$. Other parameters are same as in Fig.6. (b) A blow up of the previous figure is shown where the period doubling points are marked with arrows. Note that after each period doubling bifurcation, the system transits to a stable limit cycle (characterized by large negative σ_1) before getting unstable for the next period doubling point when σ_1 becomes close to zero. (c) The Maximal LCE in a region of pitchfork bifurcation. The first arrow (up) indicates the pitchfork bifurcation after which the system transits to a chaotic regime before becoming periodic (denoted by the negative LCE) and becomes chaotic again as α increases, following a period doubling cascade, denoted by the second arrow (down).

the maximal Lyapunov exponent σ_1 . It has also been found that the system can be completely deterministic in the middle of two chaotic regions and exhibit quasi-periodicity, as shown by the orbit diagram where a 5-period window appears in the middle of a chaotic region. We have further shown that when the parametric forcing term related to dust-charge fluctuation is small, away from the chaotic regime, the system can be driven in a frequency-locked state when a harmonic resonance of 2:1 takes place between the driving frequency and the fundamental frequency of the system. We have found that in most of the cases, the system transits to chaos through a cascade of period doubling bifurcations and the scaling of the period doubling cascades closely agrees to that of 1-D maps [24].

-
- [1] Y. Saitou Y and T. Honzawa, in *Proceedings of the Int. Cong. Plasma Phys. and 25th EPS Conf. Fusion Plasma Phys.* (Prague, Czech Republic, 1998), Vol 22, pp. 2521-2524.
[2] M. Faraday, *Phil. Trans. Royal Soc.* **20**, 299 (1831).
[3] E. Mathieu, *J. Math.* **13**, 137 (1868).
[4] A. H. Nayfeh and D. T. Mook, *Nonlinear Oscillations* (Wiley Interscience, NY, 1979).
[5] R. H. Rand, A. Barcilon, and T. M. Morrison, *Nonlin. Dyn.* **39**, 411 (2005).
[6] R. H. Rand and T. M. Morrison, *Nonlin. Dyn.* **40**, 195 (2005).
[7] R. H. Rand, A. Barcilon, and T. M. Morrison, *Nonlin. Dyn.* **39**, 411 (2005).
[8] S.-Y. Kim and B. Hu, *Phys. Rev. E* **58**, 3028 (1998).
[9] P. K. Shukla and A. A. Mamun, *Introduction to Dusty Plasma Physics* (IOP Publishing Ltd., 2002).
[10] M. R. Jana, A. Sen, and P. K. Kaw, *Phys. Rev. E* **48**, 3930 (1993).

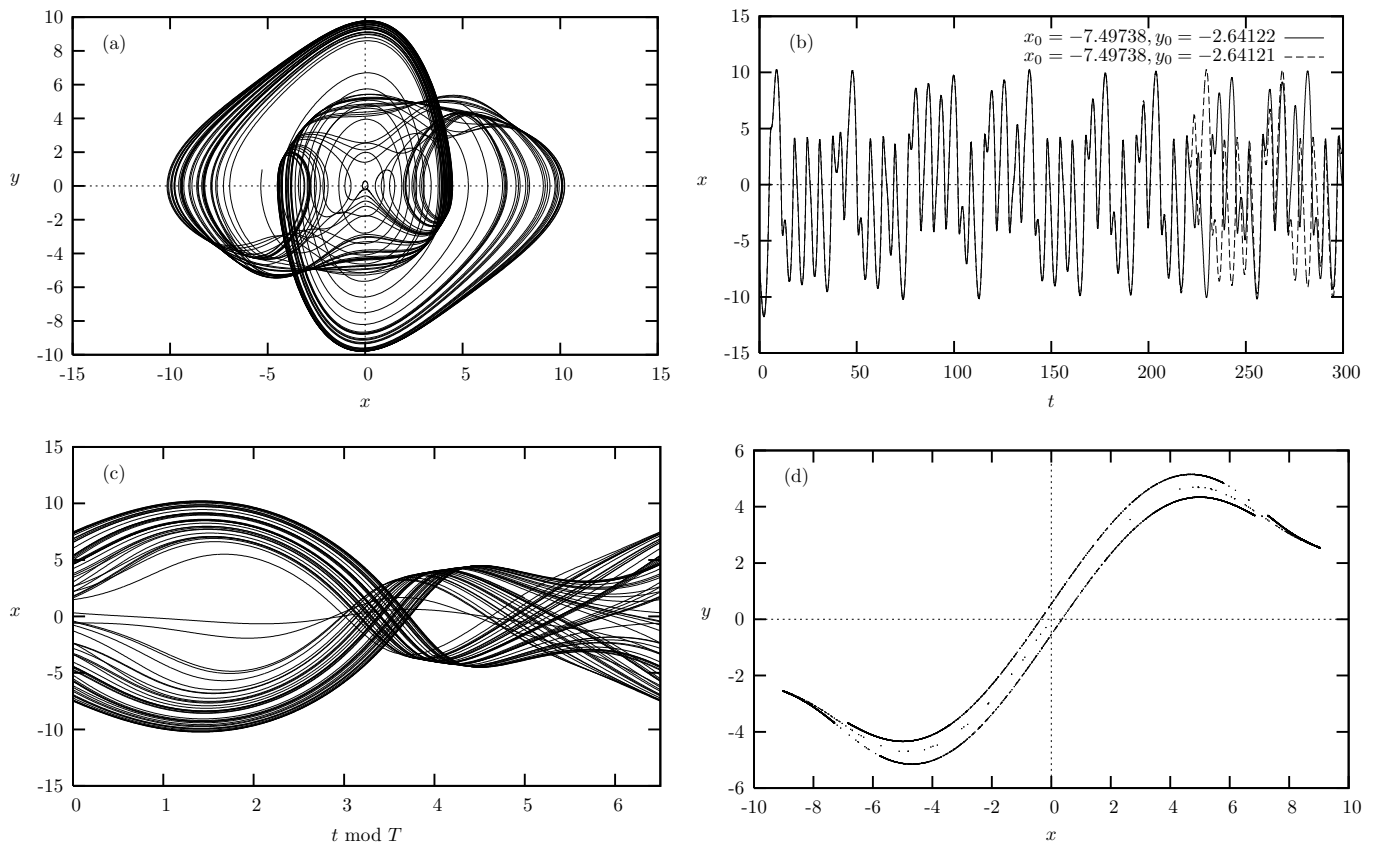


Figure 8: (a) Projection of the phase portrait in the $x-y$ plane in the chaotic regime of Eq.(10). (b) The corresponding time evolution of the variable x . Note the divergence of the two curves for change in the initial condition (x_0, y_0) at $t = 0$ at the fifth decimal place, showing the sensitivity of the system on initial conditions in the chaotic region. (c) The phase portrait in the cylindrical space $x \times y \times (t \bmod T)$, where T is the fundamental period of the system, which is 6.5 in this case. (d) The corresponding Poincaré map, which seems to fall in a fractal set, signifying chaos. The parameters in all the figures are chosen for the chaotic regime, $\alpha = 0.07$, $\epsilon = 3.41$, $\lambda = 1$, $\omega_d = 1$, and $\nu = 0.96664$ corresponding to $T = 6.5$ (refer to Fig.6).

- [11] M. Momeni, I. Kourakis, M. Moslehi-Fard, and P. K. Shukla, *J. Phys. A : Math. Theor.* **40**, F473 (2007).
- [12] D. Armbruster, M. George, and I. Oprea, *Chaos* **11**, 52 (2001).
- [13] R. Blümel, E. Bonneville, and A. Carmichael, *Phys. Rev. E* **57**, 1511 (1998).
- [14] J. Jeong and S.-Y. Kim, *J. Korean Phys. Soc.* **35**, 393 (1999).
- [15] M. Pandey, R. Rand, and A. Zehnder, in *Proceedings of Proceedings of ASME 2005 International Design Engineering Technical Conferences* (Long Beach, California, 2005), DETC2005-84018.
- [16] S. H. Strogatz, *Nonlinear Dynamics and Chaos* (Addison-Wesley, 1994).
- [17] M. Zhalutdinov *et al.*, *App. Phys. Lett.* **83**, 3281 (2003).
- [18] I. Bove, S. Boccaletti, J. Bragard, J. Kurths, and H. Mancini, *Phys. Rev. E* **69**, 016208 (2004).
- [19] J. Guckenheimer and P. Holmes, *Nonlinear Oscillations, Dynamical Systems, and Bifurcations of Vector Fields* (Springer-Verlag, NY, 1983).
- [20] J. Hale and H. Koçak, *Dynamics and Bifurcations* (Springer-Verlag, NY, 1991).
- [21] V. I. Arnold, *Ordinary Differential Equations* (MIT Press, Cambridge, 1973), pp. 114.
- [22] E. J. Doedel *et al.*, *AUTO 2000 : Continuation and Bifurcation Software for Ordinary Differential Equations*. available on line at : <http://indy.cs.concordia.ca/auto/>
- [23] B. Ermentrout, *Simulating, Analyzing, and Animating Dynamical Systems : A Guide to XPPAUT for Researchers and Students* (Cambridge, 1987).
- [24] M. J. Feigenbaum, *J. Stat. Phys.* **19**, 25 (1978); **21**, 669 (1979).
- [25] I. Shimada and T. Nagashima, *Prog. Theor. Phys.* **61**, 1605 (1979).
- [26] A. Wolf, J. B. Swift, H. L. Swinney, and J. A. Vastano, *Physica D* **16**, 285 (1985).
- [27] F. Grond *et al.*, *Chaos. Sol. Fract.* **16**, 841 (2003).